Characteristics of constrained ferroelectricity in $PbZrO_3/BaZrO_3$ superlattice films

Cheng-Lung Hung, Yu-Lun Chueh, Tai-Bor Wu,[a] and Li-Jen Chou
Department of Materials Science and Engineering, National Tsing-Hua University, Hsinchu 300, Taiwan, Republic of China

(Received 29 July 2004; accepted 17 November 2004; published online 5 January 2005)

An Artificially layered perovskite composed of antiferroelectric $PbZrO_3$ and paraelectric $BaZrO_3$ (BZO) was fabricated on $LaNiO_3/Pt/Ti/SiO_2/Si$ substrates at 475 °C by radio-frequency magnetron sputtering. It had an (001)-oriented superlattice structure with an average composition of $(Pb_{0.75}Ba_{0.25})ZrO_3$ (PBZ). X-ray diffraction, cross-sectional transmission electron microscopy, and a depth profile of a secondary-ion mass spectrometer confirmed the formation of superlattice structure with designed composition modulation. Ferroelectricity was induced in the superlattice films, and the ferroelectric as well as the dielectric properties were enhanced with reducing the stacking periodicity. The remanent polarization P_r and coercive field E_c were found linearly dependent on the applied voltage but independent of the measurement temperature up to 100 °C. The retention loss of superlattice films was small and significantly less than that of $(Pb_{1-x}Ba_x)ZrO_3$ (PBZ) solid-solution films either at room temperature or 100 °C. The dielectric constant of the superlattice films was also found insensitive to temperature up to 175 °C, but not for the PBZ solid-solution film, which exhibited a clear dielectric maximum at the Curie temperature of 125 °C. Moreover, a significant suppression of leakage current down to 10^{-8}–10^{-9} A/cm^2 was obtained in the superlattice films constructed with the wide-bandgap sublayer of BZO. © *2005 American Institute of Physics*. [DOI: 10.1063/1.1846133]

I. INTRODUCTION

Perovskite oxide thin films are attractive for application in advanced microelectronics devices such as ferroelectrics in nonvolatile memories and dielectrics in dynamic random access memories.[1] For the former application, most attention has been on two systems: $Pb(Zr_{1-x}Ti_x)O_3$ (PZT) and layered perovskites, such as $SrBi_2Ta_2O_9$ (SBT).[2] The PZT possesses a superior property of high remanent polarization.[3,4] However, the high content of oxygen vacancy in PZT, which is easy to entrap at the ferroelectric/electrode interface during polarization reversals, degrades its device lifetime and reliability.[5] In contrast, SBT[6,7] and other layered perovskites usually have an advantageous property of high resistance against polarization fatigue due to the presence of a stable $SrTaO_3$ sublayer in the structure, which has a high formation energy of oxygen vacancy and can block the oxygen migration toward the electrodes.[8] However, unlike the simple perovskite materials, such as PZT, a higher processing temperature (≧600 °C) is often required to crystallize the layered perovskite films,[9] which is detrimental for complementary metal-oxide-semiconductor compatibility and especially for the fabrication of embedded nonvolatile random access memories.[10]

The $(Pb_{1-x}Ba_x)ZrO_3$ (PBZ) with $x=0.2$–~ 0.4 is another ferroelectric material having a simple perovskite structure, which is a solid solution of antiferroelectric [$PbZrO_3$ (PZO)] and paraelectric [$BaZrO_3$ (BZO)] oxides.[11] The PBZ film has an improved property of resistance against polarization fatigue due to its less content of oxygen vacancies.[12] However, an incorporation of Pb^{4+} ions into the B-site of the perovskite lattice was found in the preparation of PBZ films, which made the films quite leaky.[13] The ferroelectric superlattice is constructed with alternating layers of different perovskites coherently grown on each other, which can be considered as an artificial layer-perovskite. Anomalous properties different from those of ordinary ferroelectric films can be sometimes obtained from the superlattice structure due to the modification of perovskite lattice by interfacial strain.[14–17] Since BZO, one of the constituents of PBZ, is a stoichiometrically stable perovskite oxide with a wide bandgap,[18] it could act as a barrier for oxygen vacancy migration and electron transport in the artificial PZO/BZO superlattice. Furthermore, as both PZO and BZO are simple perovskites, a low processing temperature can be used in fabrication of ferroelectric capacitors with such an artificially layered perovskite structure. Therefore, a series of artificial PZO/BZO superlattices with highly (001) preferred orientation was fabricated and studied in this work.

II. EXPERIMENTAL DETAILS

The PZO and BZO layers with a fixed thickness ratio of 3/1, which corresponds to an average composition of $(Pb_{0.75}Ba_{0.25})ZrO_3$, were alternately deposited on highly (001)-oriented $LaNiO_3$ (LNO) electrode.[19] The LNO electrode was coated on a $Pt/Ti/SiO_2/Si$ substrate by rf magnetron sputtering at 350 °C, and it was adopted for reducing the crystallization temperature of the perovskite oxide films.[20–22] The deposition of PZO and BZO was carried out at 475 °C by rf magnetron sputtering in an argon/oxygen (10%) ambient of 5 mTorr. Different stacking periodicities of PZO/BZO

[a]Electronic mail: tbwu@mse.nthu.edu.tw

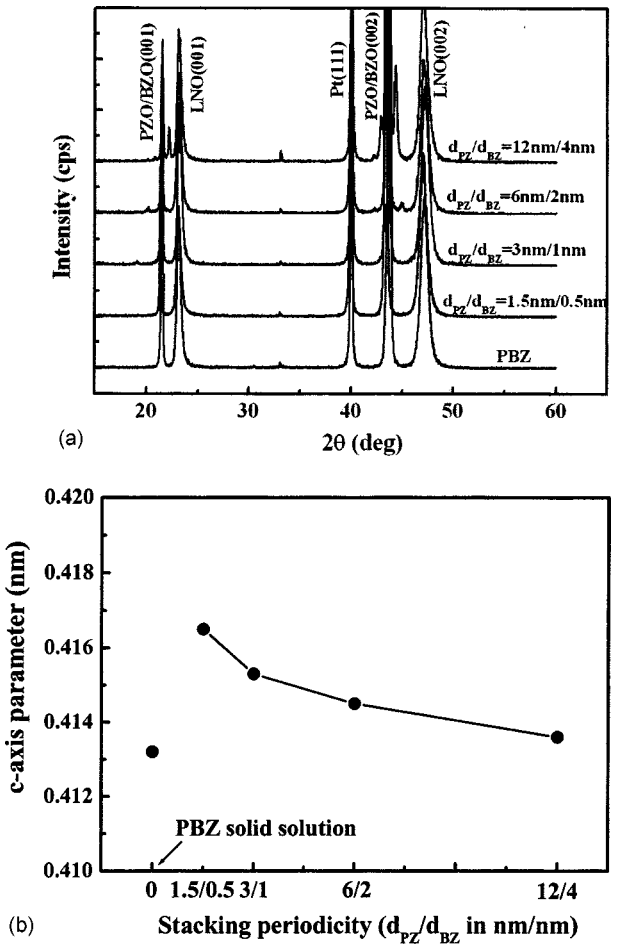

FIG. 1. (a) XRD patterns, and (b) the change in the mean c-axis parameter as a function of stacking periodicity of the PZO/BZO superlattices.

in the range from 1.5 nm/0.5 nm to 12 nm/4 nm were adopted. The total thickness of the resulting films was ~120 nm. For a comparison, a solid-solution PBZ film of the same composition and thickness was also prepared. X-ray diffraction (XRD) with Cu K_α radiation was carried out to identify the crystalline structure of the films. High-resolution transmission electron microscopy (HRTEM) was employed to observe the cross-sectional structure of the superlattice. Additionally, the composition depth profile was examined with the secondary-ion mass spectrometer (SIMS). To measure the electrical properties, a Pt top electrode was deposited onto the films. Ferroelectric properties, including polarization-electric field (P-E) hysteresis and retention test, were measured at temperatures ranging from room temperature to 175 °C with a RT66A test system (Radiant Technology), operating in the virtual ground mode. The dielectric property at the aforementioned temperatures was also examined with HP4192 at the frequencies of 1 kHz and 1 MHz. The leakage-current characteristic was measured at RT with an HP4140B pA meter/dc voltage source.

III. RESULTS AND DISCUSSION

Figure 1(a) shows the XRD patterns of the PBZ and the artificially layered PZO/BZO films. All the films have the same strong (001)-oriented structure as that of the LNO electrode due to the lattice-coherent growth of the films on LNO.[20–22] The formation of a superlattice structure was identified from the appearance of satellite peaks around the main diffraction peak of the PZO/BZO films. The stacking periodicity calculated from the satellite peak intervals agrees, in general, with the designed value. It is also noticed that the satellite peaks gradually became indistinct with decreasing the stacking periodicity, indicating the presence of composition intermixing at the interfaces between PZO and BZO.[23] The change of lattice parameter c evaluated from the main diffraction peak position of the superlattice films is shown in Fig. 1(b). It increases with the decrease of stacking periodicity, and all the films have larger lattice spacing in the normal direction (*c* axis) than that of the PBZ solid-solution film. The result is similar to that of the BTO/STO superlattice, which has been attributed to the in-plane coherency strain induced from the larger lattice mismatch between the heteroepitaxial layers in the superlattice.[14,15] The composition modulation obtained from the SIMS depth profile of a PZO/BZO film shown in Fig. 2 also reveals the high periodic uniformity in intensity and pitch of the repetitive layers.

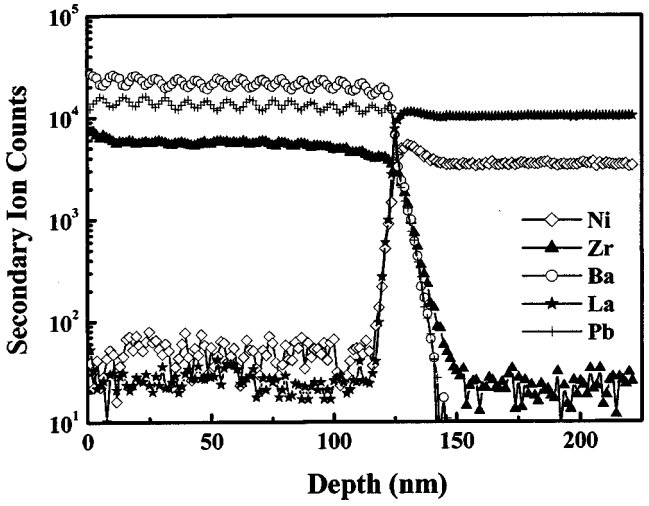

FIG. 2. The SIMS depth profile of $[PZO(6\ nm)/BZO(2\ nm)]_{15}$/LNO film.

The superlattice structure was then examined by HRTEM. Figure 3(a) displays the cross-sectional image of a $[PZO(6\ nm)/BZO(2\ nm)]_{15}$ multilayer on LNO electrode. The stacking periodicity calculated from the image is consistent with the designed value. The contrast of PZO layers appears more obscure than that of the BZO layers and the layers are distinctly separated from each other. The differ-

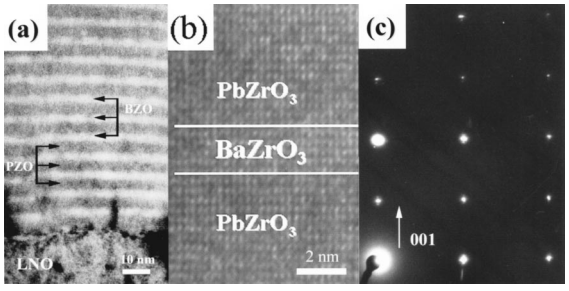

FIG. 3. (a) The cross-sectional image, (b) lattice image, and (c) electron diffraction pattern of $[PZO(6\ nm)/BZO(2\ nm)]_{15}$ superlattice.

ence in contrast is possibly caused by a stronger diffraction of the Pb atoms in comparison to the Ba atoms. The lattice image of the PZO/BZO stacks was further obtained and shown in Fig. 3(b). A clear coherency of lattice between the sublayers could be observed, which confirms the pseudomorphic growth in the artificially layered structure. A selected-area electron diffraction (SAED) pattern taken from the area including both PZO and BZO layers is shown in Fig. 3(c), which was recorded with the electron-beam direction parallel to the [110] zone axis of the LNO substrate. The shape of diffraction spots is identified to be a superposition of [001]-zone SAED patterns of tetragonal $PbZrO_3$ and cubic $BaZrO_3$. Additionally, it indicates that *a* axes and *b* axes of tetragonal $PbZrO_3$ lie in the plane of the interface, and that the *c* axis is parallel to the growth direction.

All the PZO/BZO superlattice films exhibit ferroelectric characteristic as that of the PBZ film, although it is suppressed with increasing the stacking periodicity, as observed from the P-E hysteresis curves shown in Fig. 4(a). The change of remanent polarization P_r and coercive field E_c with respect to the applied voltage are depicted in Fig. 4(b). It is interesting to see that both P_r and E_c values increase linearly from zero axes with the applied voltage for all the superlattice films. This "linear" characteristic of ferroelectricity is different from the nonlinear relation normally observed with the ferroelectric films, such as that of PBZ films shown in the same figure. The results from high-temperature measurement further reveal ferroelectric characteristics of the PZO/BZO superlattice different from that of PBZ solid-solution film. As illustrated in Fig. 5, the same linearity [Fig. 5(a)] with temperature-independent P_r and E_c values [Fig. 5(b)] can be observed for the PZO/BZO superlattice upon raising the temperature up to 100 °C, but the values of PBZ film decreased by $\sim$ 15%. However, the low-voltage ferroelectricity of the superlattices became gradually lost upon increasing temperature over 100 °C, observed by the result of PZO(1.5 nm)/BZO(0.5 nm) shown in Fig. 6. It should be pointed out that the P-E hysteresis curves obtained under applied voltage above 10 V were quite lossy at temperatures $\geqslant$150 °C due to the large increase of leakage current, which distorted the measured P_r and E_c values, and thus, they are not included in the figure. A similar but worse result of lossy ferroelectricity was observed from the PBZ film at temperatures $\geqslant$125 °C.

The P-E hysteresis behavior of ferroelectric materials is related to the reorientation of spontaneous polarization (or its domains) by an applied electric field. It takes place rapidly at the coercive field, and slows down while approaching the saturation state with increasing the applied field, giving rise to the normally observed nonlinear increase of remanent polarization with respect the applied voltage. Moreover, the reorientation of polarization or the domain alignment would be disturbed by thermal agitation, causing the decrease of P_r and E_c values with increasing the measurement temperature, which is the typical polarization relaxation behavior in normal ferroelectric material.[24,25] Therefore, the linear and temperature-independent characteristics of ferroelectricity observed here in the PZO/BZO superlattice film are unusual. They must be related to the constraint of PZO structure from

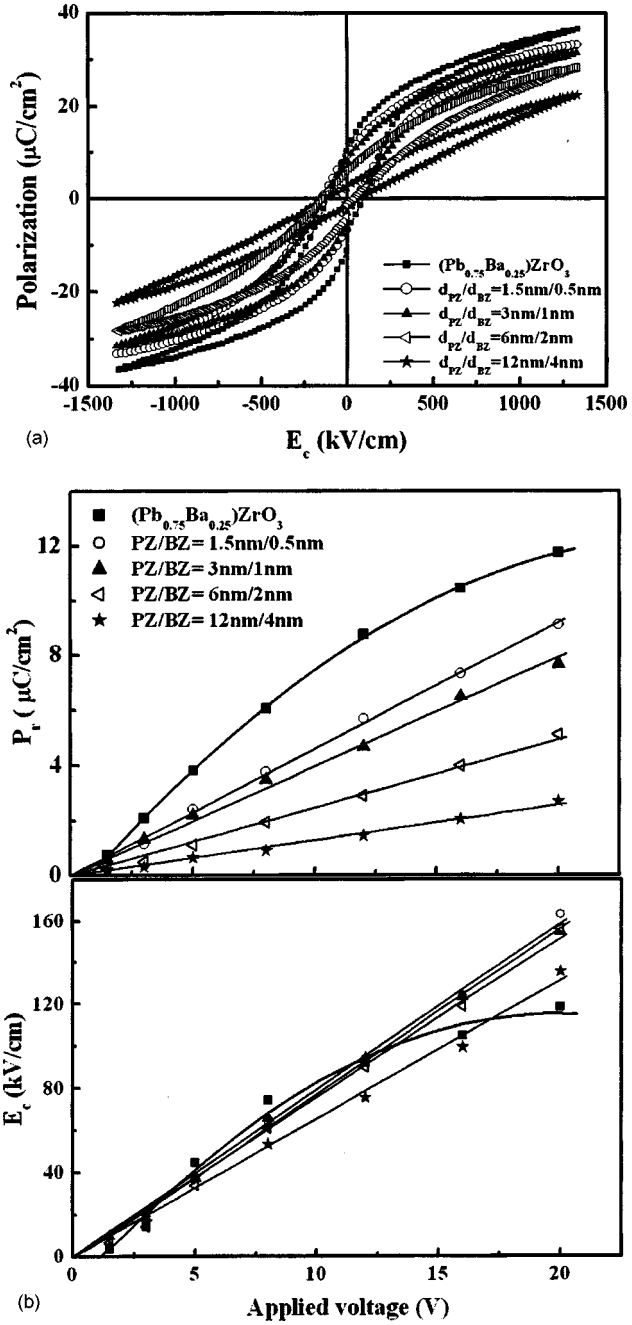

FIG. 4. (a) P-E hysteresis loops and (b) change of remanent polarization P_r and coercive field E_c with respect to the applied voltage, on the PBZ and PZO/BZO superlattice films having different stacking periodicities and measured at RT.

the BZO sublayers with respect to lattice coherency. For an antiferroelectric material of PZO, the ferroelectric phase can be induced by electric or mechanical stress,[26,27] and in the PZO/BZO superlattice, the in-plane coherency strain brought from the BZO sublayer with a larger lattice has apparently caused the transition of PZO layers from antiferroelectric into ferroelectric state, providing the ferroelectricity of the superlattice. On the other hand, the paraelectric layer of BZO would also act as a constraint against the reversal of spontaneous polarization in the ferroelectric layer of PZO, as discussed in the following.

For an applied voltage, V_a, in the layered structure of

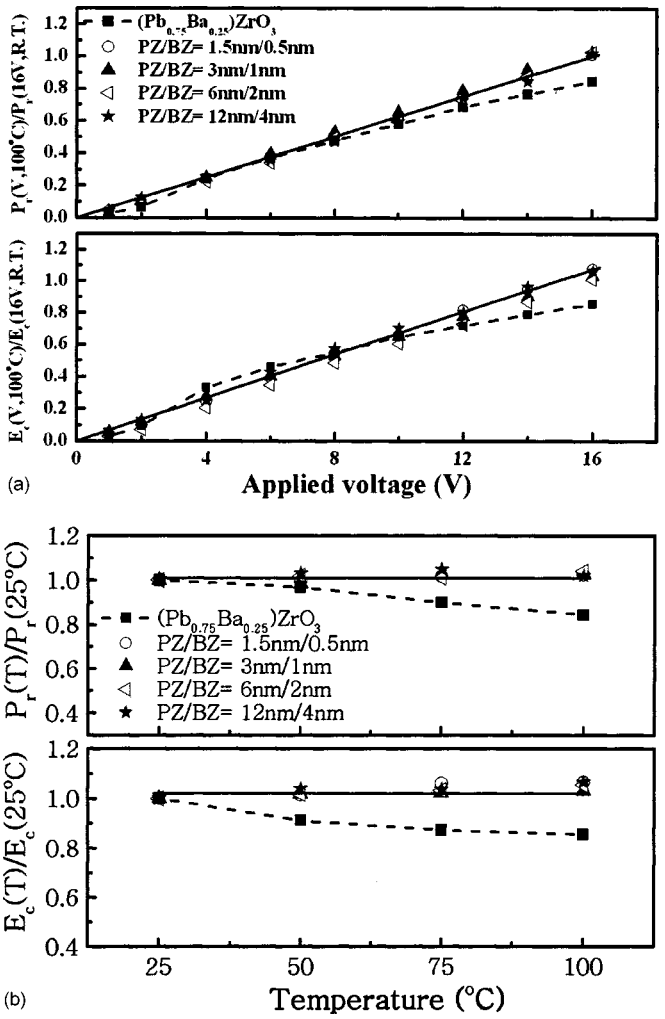

FIG. 5. (a) The voltage dependence of remanent polarization P_r and coercive field E_c at 100 °C relative to those measured at 16 V and RT, and (b) the change of P_r and E_c values against measurement temperature at 16 V of applied voltage.

PZO/BZO, the electrostatic energy E, gained from dielectric polarization and spontaneous polarization reversal can be expressed as

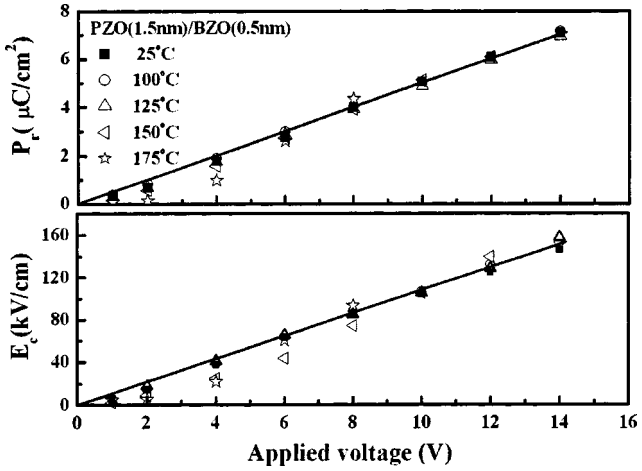

FIG. 6. The change of remanent polarization P_r and coercive field E_c in the PZO (1.5 nm)/BZO(0.5 nm) film measured at temperatures above 100 °C, as a function of applied voltage.

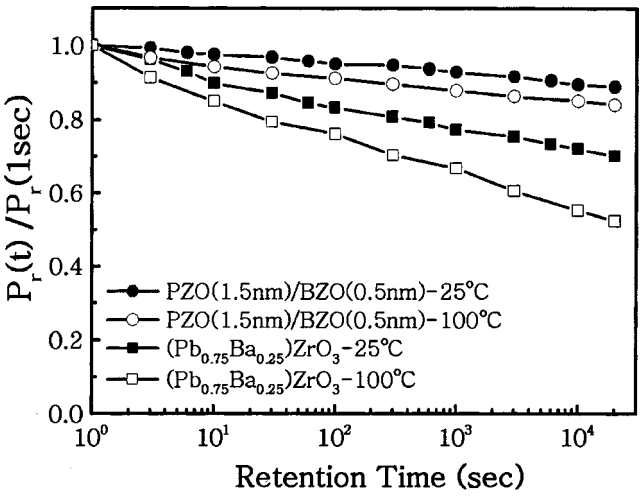

FIG. 7. Retention characteristics of PZO(1.5 nm)/BZO(0.5 nm) superlattice and PBZ films measured at RT and 100 °C.

$$E = 1/2(C_p V_p^2 + C_f V_f^2) - P_f V_f, \tag{1}$$

where C_p, V_p and C_f, V_f are the capacitance and voltage components of the paraelectric layer (BZO) and ferroelectric layer (PZO), respectively, and P_f is the amount of polarization reversal in the ferroelectric layer. Since $V_p + V_f = V_a$, and $C_p V_p = C_f V_f + P_f$, an equilibrium state of polarization switching can be achieved at the condition of $(\partial E/\partial P_f)_{V_a} = 0$, which gives the constraint of polarization reversal, P_f^e, in the ferroelectric layer before reaching the saturation state:

$$P_f^e = 1/3 C_p V_a. \tag{2}$$

It is interesting to see that the constrained polarization P_f^e is linearly proportional to the applied voltage, and determined by the capacitance of paraelectric layer C_p. For a stable paraelectric material of BZO, its permittivity is insensitive to temperature, and, from Eq. (2), the constrained polarization will be also insensitive to temperature. Therefore, the linear and temperature-independent characteristics of ferroelectricity in the PZO/BZO superlattices can be realized, since the P_r and E_c values are related to the preservation and elimination of the constrained polarization, respectively.

Figure 7 shows the retention characteristics of PBZ and PZO (1.5 nm)/BZO (0.5 nm) superlattice films measured at RT and 100 °C. The test was performed under write and read voltages of 16 V. As shown in the figure, the remanent polarization in PBZ and superlattice films decreased with increasing the retention time up to 2×10^4 s. The degradation of polarization in PBZ film is ~30% at RT and significantly increases to ~52% at 100 °C. However, that of superlattice film is only ~12% at RT and increases slightly to ~16% at 100 °C. The polarization loss in retention is usually attributed to the depolarization field induced from space charges.[28] The space-charged layers at the metal/ferroelectric interface are formed from the segregation of oxygen vacancies, which cause the increase of depolarization field, resulting in an increase of polarization loss.[29] The segregation of oxygen vacancies would be accelerated at high temperature and, thus, significantly enhance the degradation of polarization in the PBZ films. However, the polarization degradation in the ar-

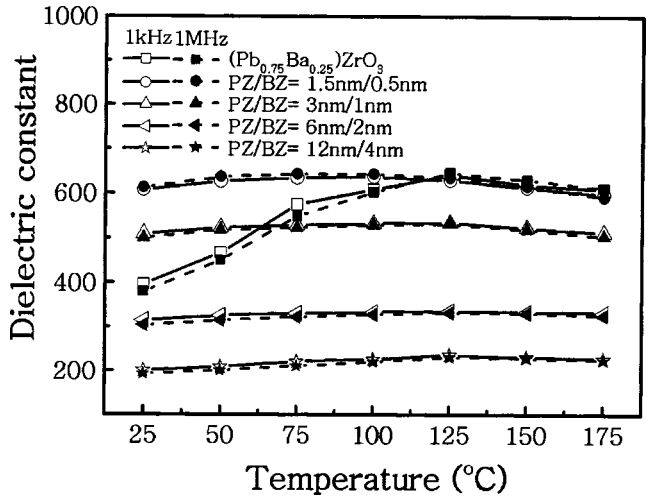

FIG. 8. The dielectric constant of PBZ and superlattice films measured at frequency of 1 kHz and 1 MHz and temperatures from RT to 175 °C.

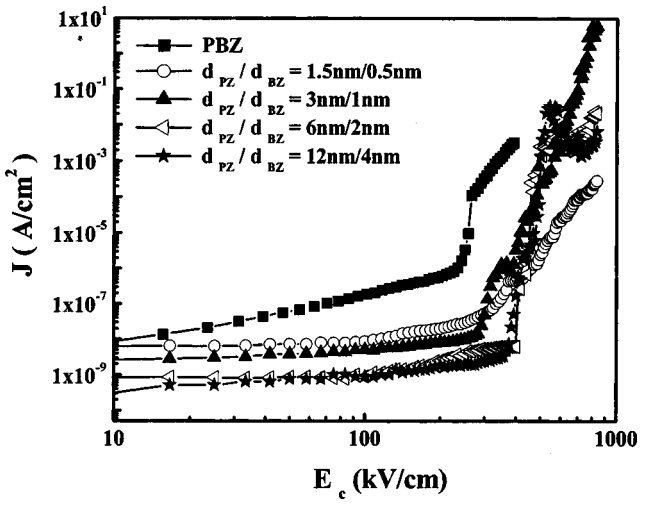

FIG. 9. Leakage-current characteristics of the PBZ and PZO/BZO superlattice films.

tificial PZO/BZO superlattice is comparable to that of $SrBi_2Ta_2O_9$ layered perovskite film, which has a stable $SrTaO_3$ sublayer to block oxygen migration toward the electrodes.[8] The stable BZO layer in the superlattices obviously has a similar effect on blocking the migration of oxygen vacancies and, thereby, leads to the good retention property.

The superlattice films also have dielectric characteristics different from that of PBZ solid-solution films. Figure 8 shows the change of dielectric constant of PBZ film and superlattices having different periodicities upon raising the measurement temperature from RT to 175 °C at frequencies of 1 kHz and 1 MHz. It can be seen that the superlattice films have a higher dielectric constant with decreasing the stacking periodicity, and all the films have an insignificant frequency dependence of dielectricity. The enhancement of dielectric property in association with the expansion of c-axis lattice spacing observed previously in the superlattice films is undoubtedly related to the lattice softening induced by the in-plane coherency strain between the heteroepitaxial layers of PZO and BZO with reducing the stacking periodicity.[14,15] It is also interesting to notice that the dielectric constant of PBZ film greatly increases with raising the measurement temperature before reaching the maximum at the Curie temperature of transition from ferroelectric to paraelectric phase in $(Pb_{0.75}Ba_{0.25})ZrO_3$, i.e., ~125 °C,[30] but that of superlattice films changes only insignificantly, with an indistinct maximum at temperature around 100–~125 °C.

In normal ferroelectric materials, the dielectric constant drastically increases when approaching the Curie temperature due to the softening of lattice in relation to the structural change in phase transition between ferroelectric and paraelectric. Such a temperature dependence of dielectric constant was indeed observed in the PBZ, but not in the superlattice films. This temperature insensitivity of dielectric constant can also be realized by the constraint against structural change in the PZO layer from the paraelectric layer of BZO to maintain the lattice coherency. In other words, the incorporation of the BZO sublayer in the PZO/BZO superlattice not only induces the ferroelectric phase but also stabilizes the corresponding structure against thermal agitation. As for the indistinct dielectric maximum observed in Fig. 8, it is probably due in part to the relaxation of constrained structure in the region near the incoherent interface with the Pt electrode, which may also explain the loss of low-voltage ferroelectricity at temperatures beyond 100 °C, as observed previously in Fig. 6.

The characteristic of current density J versus electric field E in the PZO/BZO superlattices and that of the PBZ film are also shown in Fig. 9. All the superlattice films are highly insulating with leakage current of 10^{-8}–~10^{-9} A/cm^2 at a field of 300 kV/cm, which is significantly lower not only than that of PBZ but also that of PZT[31] or SBT,[32] although it increases, in general, with decreasing the BZO sublayer thickness. The result clearly exhibits another advantage of constructing the ferroelectric superlattice with a wide-bandgap BZO sublayer in order to suppress the leakage current.

IV. CONCLUSIONS

An artificially layered perovskite of PZO/BZO was prepared, which had an (001)-oriented superlattice structure consisting of antiferroelectric PZO and paraelectric BZO sublayers with an average composition of $(Pb_{0.75}Ba_{0.25})ZrO_3$, and which was grown on the LNO/Pt/Ti/SiO_2/Si substrates at 475 °C by rf magnetron sputtering. The XRD and HRTEM confirmed the formation of superlattice structure with designed composition modulation. It was found that the decrease of stacking periodicity would increase the mean *c*-axis parameter of the superlattice and would thus lead to an enhancement of dielectric and ferroelectric properties. A linear increase of remanent polarization P_r and coercive field E_c against applied voltage was found in the superlattice films, but not in the PBZ solid-solution film. This "linear" ferroelectricity is independent of measured temperature up to 100 °C. The retention of ferroelectric property was also greatly improved in the superlattice films, either that at RT or at 100 °C. The superlattice films show a temperature-insensitive dielectricity, which is very different from that of

the PBZ films. A model of constrained polarization was proposed to explain the observed linear and temperature-independent characteristics of the PZO/BZO superlattices. Moreover, the leakage current was significantly suppressed in the superlattice films constructed with the wide-bandgap sublayer of BZO.

ACKNOWLEDGMENT

The authors gratefully acknowledge the support by the Ministry of Education of Republic of China under Contract Number A-91-E-FA04-1-4.

[1]M. Suzuki and T. Ami, Mater. Sci. Eng., B **41**, 166 (1999).
[2]Z. G. Zhang, J. S. Liu, Y. N. Wang, J. S. Zhu, F. Yan, X. B. Chen, and H. M. Shen, Appl. Phys. Lett. **73**, 788 (1998).
[3]J. Chen, M. P. Harmer, and D. M. Smith, J. Appl. Phys. **76**, 5394 (1994).
[4]W. L. Warren, D. Dimos, B. A. Tuttle, R. D. Nasby, and G. E. Pike, Appl. Phys. Lett. **65**, 1018 (1994).
[5]J. J. Lee, C. L. Thio, and S. B. Desu, J. Appl. Phys. **78**, 5073 (1995).
[6]C. A. Araujo, J. D. Cuchiaro, L. D. McMillan, M. C. Scott, and J. F. Scott, Nature (London) **374**, 627 (1995).
[7]R. Dat, J. K. Lee, O. Auciello, and A. I. Kingon, Appl. Phys. Lett. **67**, 572 (1995).
[8]B. H. Park, S. J. Hyun, S. D. Bu, T. W. Noh, J. Lee, H.-D. Kim, T. H. Kim, and W. Jo, Appl. Phys. Lett. **74**, 1907 (1999).
[9]G. D. Hu, I. H. Wilson, J. B. Xu, C. P. Li, and S. P. Wong, Appl. Phys. Lett. **76**, 1758 (2000).
[10]K. Amanuma, T. Hase, and Y. Miyasaka, Appl. Phys. Lett. **66**, 221 (1995).
[11]G. Seirnet, Phys. Rev. **86**, 219 (1952).
[12]J. H. Tseng and T. B. Wu, Appl. Phys. Lett. **78**, 1721 (2001).
[13]T. B. Wu and J. H. Tseng, Key Eng. Mater. **214–215**, 133 (2002).
[14]H. Tabata, H. Tanaka, and T. Kawai, Appl. Phys. Lett. **65**, 1970 (1994).
[15]J. Kim, Y. Kim, Y. S. Kim, J. Lee, L. Kim, and D. Jung, Appl. Phys. Lett. **80**, 3581 (2002).
[16]L. Kim, D. Jung, J. Kim, Y. S. Kim, and J. Kee, Appl. Phys. Lett. **82**, 2118 (2003).
[17]T. Shimuta, O. Nakagawara, T. Makino, S. Arai, H. Tabata, and T. Kawai, J. Appl. Phys. **91**, 2290 (2002).
[18]J. Robertson, J. Vac. Sci. Technol. B **18**, 1785 (2000).
[19]M. S. Chen, T. B. Wu, and J. M. Wu, Appl. Phys. Lett. **68**, 1430 (1996).
[20]T. B. Wu, J. M. Wu, C. M. Wu, M. J. Shyu, M. S. Chen, J. S. Dong, and C. C. Yang, Mater. Res. Soc. Symp. Proc. **433**, 169 (1996).
[21]C. H. Lin, B. M. Yen, H. C. Kuo, H. Chen, T. B. Wu, and G. E. Stillman, J. Mater. Res. **15**, 115 (2000).
[22]S. L. Lung, C. L. Liu, S. S. Chen, S. C. Lia, C. W. Tsai, T. T. Sheng, T. Wang, S. Pan, T. B. Wu, and R. Liu, Tech. Dig. - Int. Electron Devices Meet. 2001, 275.
[23]Y. Ishibashi, N. Ohashi, and T. Tsusumi, Jpn. J. Appl. Phys., Part 1 **39**, 186 (2000).
[24]F. Xu, S. T. Mckinstry, W. Ren, B. Xu, Z.-L. Xie, and K. J. Hemker, J. Appl. Phys. **89**, 1336 (2001).
[25]H. Maiwa, S. H. Kim, and N. Ichinose, Appl. Phys. Lett. **83**, 4396 (2003).
[26]S. S. N. Bharadwaja and S. B. Krupanidhi, J. Appl. Phys. **89**, 4541 (2001).
[27]J. Zhai, Y. Yao, X. Li, T. F. Hung, Z. K. Xu, H. Chen, E. V. Colla, and T. B. Wu, J. Appl. Phys. **92**, 3990 (2002).
[28]R. R. Metha, B. D. Silverman, and J. T. Jacobs, J. Appl. Phys. **44**, 3379 (1973).
[29]S. N. Ryoo, S. G. Yoon, and S. H. Kim, Appl. Phys. Lett. **83**, 2880 (2003).
[30]B. P. Pokharel and D. Pandey, J. Appl. Phys. **88**, 5364 (2000).
[31]G. C. Chao and J. M. Wu, Jpn. J. Appl. Phys., Part 1 **40**, 1306 (2001).
[32]W. C. Shin and S. G. Yoon, Appl. Phys. Lett. **79**, 1519 (2001).